Effect of Residual Dipolar Interactions on the NMR Relaxation in Cross-Linked Elastomers

P. Sotta,[†,§] C. Fülber,[†,‡] D. E. Demco,[†] B. Blümich,[‡] and H. W. Spiess*[,†]

Max-Planck-Institut für Polymerforschung, Ackermannweg 10, Postfach 3148, 55021 Mainz, Germany, and Institut für Makromolekulare Chemie, RWTH Aachen, Worringerweg 1, 52056 Aachen, Germany

Received January 30, 1996; Revised Manuscript Received June 4, 1996[⊗]

ABSTRACT: For elastomer networks above the glass transition temperature T_g, a unified approach is presented to relate the residual dipolar couplings in various independent NMR experiments to the cross-link density. This is demonstrated on a series of cross-linked poly(styrene-*co*-butadiene) elastomers. The presence of dynamic physical and permanent chemical cross-links leads to a nonzero average of the homonuclear and heteronuclear dipolar couplings, which results in a solid-like NMR relaxation behavior. The residual dipolar couplings are expressed as a function of the effective number of statistical segments N_e between the physical and N_e^X between the chemical cross-link points, using a simplified network model with Gaussian statistics. These effective numbers are extracted for each sample of the series from the ^{13}C-edited transverse ^1H magnetization relaxation of the CH group. It is shown that the respective N_e values can be used to scale the time domain of various NMR experiments such as (a) the free induction decay, (b) the ^{13}C-edited ^1H transverse magnetization relaxation, (c) the cross-polarization curves, and (d) the ^1H magnetization exchange between the CH and CH_2 groups. This proves the validity of the unified view on the dipolar interactions in elastomer networks and provides a way to estimate the cross-link density.

I. Introduction

Cross-linking of technical elastomers such as poly(styrene-*co*-butadiene) (synthetic rubber, SBR) is of crucial importance for the mechanical properties of rubber products. Therefore, these materials, either filled or unfilled, have been the subject of a large number of NMR investigations aimed at relating the microscopic chain behavior to the macroscopic properties.[1−6] From the viewpoint of NMR, cross-linked elastomers exhibit both solid- and liquid-like features. At temperatures well above the glass transition temperature T_g, the time scales and amplitudes of molecular motions are liquid-like. However, the chain motion is not isotropic, which leads to a nonzero average of anisotropic spin interactions, such as dipole−dipole couplings, thus giving rise to solid-like properties.[7−11] Restrictions to the chain motions result from local chain order, for example due to the presence of extended conformations or stiffening elements on a short length scale, and entanglements as well as permanent chemical cross-links on a larger scale. The former are also present in a polymer melt, and the last is characteristic of elastomers. It is natural to treat the residual couplings resulting from chemical cross-links and entanglements by statistical chain models.[4] On the other hand, treating the local chain order requires a detailed knowledge of the molecular structure. However, for simplicity, we treat the local order as if it would result from the presence of physical cross-links on a smaller scale. Then this allows us to express all contributions in terms of effective mesh sizes. Depending on the degree of motional restrictions, these residual dipolar interactions may be quite small compared to those in rigid solids. Note that in deuterated systems, the same concept applies to quadrupolar interactions as well.[12−14]

These residual dipole−dipole couplings are reflected in different ways in various NMR parameters. However, a unified approach is missing for a consistent analysis of such data. The purpose of this work is, therefore, to analyze the effect of the cross-link density on several proton (^1H) or carbon (^{13}C) NMR parameters reflecting residual dipolar interactions in a series of vulcanized industrial poly(styrene-*co*-butadiene) elastomers (SBR) with different cross-link densities. Specifically, the following NMR observables have been considered: (1) the 2D ^1H exchange spectrum with a short mixing time, (2) the ^1H transverse relaxation obtained in a solid−echo pulse train, (3) the ^1H transverse relaxation obtained in a spin−echo pulse sequence, (4) the ^{13}C-edited ^1H transverse relaxation, (5) the rate of ^1H magnetization exchange between CH and CH_2 groups, and (6) the rate of magnetization transfer from ^1H to ^{13}C in a cross-polarization (CP) experiment.

Some attempts have recently been made to correlate $^1H-^{13}C$ cross-polarization rates to the cross-link density in elastomers, as reflected in a viscoelastic property (namely, the shear modulus).[15,16] Yet, this correlation was essentially empirical and was not based on a specific model of polymer chain behavior in a cross-linked system. Here we use a variety of NMR techniques which probe the partially averaged interactions. The various NMR observables, analyzed within the same theoretical framework, provide a quantitative characterization of the densities of both chemical and physical cross-links in a series of samples which differ only in cross-link density. On a microscopic scale, the NMR behavior is related to the average chain length between both chemical and physical cross-links, expressed by an average effective number of statistical segments N_e. On a macroscopic scale, it is correlated to the maximum vulcameter torque or shear modulus for the cross-link series. Thus, relations between the different NMR observables and viscoelastic properties are established. Then the NMR technique most ap-

* To whom correspondence should be addressed.
† Max-Planck-Institut für Polymerforschung.
‡ Institut für Makromolekulare Chemie.
§ Permanent address: Laboratoire de Physique des Solides, Université Paris-Sud (CNRS LA 002), Bat. 510, 91405 Orsay Cedex, France.
⊗ Abstract published in *Advance ACS Abstracts,* August 1, 1996.

S0024-9297(96)00141-6 CCC: $12.00

propriate for a specific aspect of elastomer behavior may be chosen.

The paper is organized as follows. The model which provides the framework of the present analysis is recalled in section II. A very simple description of the NMR properties of elastomer chains is adopted. Samples and experimental procedures are described in section III, and the results are presented in section IV. First, the validity of the assumptions made about the time scales of the different motions in the system are checked by appropriate two-dimensional and time-domain NMR experiments. The spin interactions involved in the different NMR experiments are specified. As the model leads to an extremely simple scaling property in the time domain, a master curve including all the samples in the series is drawn for each experiment by scaling the time axis with the respective value of the number of segments N_e.

II. NMR Properties of Polymer Chains in Elastomers

The properties of cross-linked chains which lead to a solid-like NMR behavior are reviewed in this section. The main point is that any anisotropic spin interaction fixed to a chain segment has a nonzero motional-average value due to the constraints imposed by interactions between chains in the bulk and by cross-link junctions. Specifically, the chain motion probed by a local second-rank tensorial interaction exhibits a finite order parameter $\langle P_2 \rangle$. A hierarchy of $\langle P_2 \rangle$'s can be envisaged on different time scales.[12] In polymer melts, $\langle P_2 \rangle$'s have transient values, whereas in elastomers, the cross-link points make them permanent.[17]

Dipolar spin−spin interactions are considered specifically here. One has to distinguish interactions between two nuclei located on the same segment (or, in other words, with a fixed distance) and interactions between nuclei located on different segments. The former are averaged by rotational motions, while the latter, in addition, can undergo translational diffusion which further reduces the dipolar couplings. It is supposed here that the couplings resulting from such remote interactions are much smaller than those associated with close interactions. Therefore, remote couplings are not treated explicitly, and we are left with a system of quasi-isolated interacting groups of spins, which carry a nonzero average interaction.

II.1. Residual Dipolar Interactions. Cross-link points prevent overall translational diffusion of the chains. They are treated here as points with fixed average positions, because their fluctuations are considered to be fast on the NMR time scale. We consider long, flexible chains attached to fixed cross-link points, which in the real systems are randomly spaced along the chains. In what follows, we use the term "chain" to refer to any portion of the initial polymer chains connecting two consecutive cross-link points. The effect of dangling ends is neglected. Entanglements are discussed later on.

The simplest model to describe chain statistics from the NMR point of view is a chain of freely jointed segments of fixed length.[18] Such a chain may be rescaled in several hierarchical steps according to the time scale of the motions which take place at different spatial scales, compared to the time scale defined by the NMR spin interactions. All intrachain motions are assumed to be fast enough to average elementary interactions, whereas junction average positions are static.[8]

Let us consider a linear chain of N statistical segments, fixed at its extremities. An average orientation is induced along the chain by these constraints. To estimate the effect of this average orientation on NMR properties, the most simple picture is to consider that each segment carries an isolated pair of spins separated by a distance r_{IJ} (two-spin approximation). The dipolar Hamiltonian is given by[19]

$$H_{IJ} = \omega_{IJ}(\vartheta)(3I_zJ_z - \vec{I}\cdot\vec{J}) \tag{1}$$

with the spatial part of the interaction:

$$\omega_{IJ}(\vartheta) = -\Delta_{IJ}\frac{3\cos^2\vartheta - 1}{2} \tag{2}$$

where ϑ denotes the angle between the vector connecting the spins and the steady magnetic field. The coupling strength, Δ_{IJ}, is defined as

$$\Delta_{IJ} = \frac{\mu_0}{4\pi}\frac{\gamma_I\gamma_J\hbar}{r_{IJ}^3} \tag{3}$$

and γ_i's are the magnetogyric ratios for each nucleus. Fast, liquid-like intrachain motions average this interaction. However, due to the constraints, the residual value is not zero, because some degree of anisotropy of the motions is induced along the end-to-end vector $\vec{R}$. The residual dipolar interaction within the chain may be expressed as[8,20]

$$\overline{\omega_{IJ,\vec{R}}} = \Delta_{IJ}\frac{k}{N^2a^2}\vec{R}^2\frac{3\cos^2\Theta - 1}{2} = \Delta_{IJ}\frac{k}{N^2a^2}\frac{2z^2 - x^2 - y^2}{2} \tag{4}$$

where (x,y,z) are the components of the end-to-end vector, so that $\vec{R}^2 = x^2 + y^2 + z^2$, Θ is the angle between $\vec{R}$ and the magnetic field, and a is the length of a statistical segment. The geometrical factor k depends on the model which is adopted to describe the chain statistics. It is equal to $^3/_5$ for a chain of freely jointed segments, for instance.[14] On the other hand, for a quantitative comparison to actual polymer chains under consideration, the local geometry and dynamics, as well as limited chain flexibility, have to be taken into account. Therefore, the parameter N is not in fact the actual number of repeat units between cross-links, but is proportional to it. Thus, at this point, all details of the particular spin interactions which depend on the local structure of the chain monomers are included in the factor k.

The parameter N describes the effect of the long- or medium-range structure, e.g. the cross-link density, on the NMR interactions. The mean-squared end-to-end vector is $\vec{R}^2 \approx Na^2$, and thus the residual interaction $\overline{\omega_{IJ,\vec{R}}}$ in eq 4 scales as N^{-1}. It is this property which is used in what follows, and there are no additional constraints applied to the chains in this model. The residual interaction is therefore homogeneously distributed along the chain, which is of course not exactly the case in real samples.[21]

The residual dipolar interaction manifests itself as a common property for the different NMR experiments presented here. The effect of fast motions is to effectively average the couplings between remote groups, which leads to the two-spin approximation. Thus, the

above statements and eq 4 hold for any spin pair interaction bound to the chain segment, with a fixed internuclear distance r (included in the quantity Δ in eq 4). Within this framework, the time evolution of the transverse magnetization (FID) for a spin pair in the chain may be written in the very simple form

$$M_{\vec{R}}(t) = M_0 e^{-t/T_2} \cos \overline{\omega_{\vec{R}}} t = \mathrm{Re}[M_0 e^{-t/T_2} e^{i\overline{\omega_{\vec{R}}} t}] \quad (5)$$

The cosine term represents the solid-like contribution, related to the nonzero average value of the dipolar Hamiltonian. Static, nonzero interactions, even though they may be very weak as compared to a true solid system, lead to a coherent, or reversible time evolution, which can be refocused by appropriate pulse sequences. In the frequency domain, the line shape is inhomogeneously broadened by these interactions.[19] The T_2 term is related to the fluctuating part of the Hamiltonian and corresponds to the homogeneous broadening of the line. At temperatures high enough above T_g, the T_2 contribution in eq 5 evolves generally slower than the solid-like term, so that, for the time being, the homogeneous broadening may be neglected.[22]

Of course, the coherent oscillations associated with the cosine term in eq 5 are not observed here because the systems investigated are considerably disordered. To model this disorder, the end-to-end vector components may be supposed to obey ideal, Gaussian statistics, with a normalized distribution for end-to-end vectors:[14]

$$P(\vec{R})\, \mathrm{d}\vec{R} = \left(\frac{3}{2\pi N a^2}\right)^{3/2} \exp\left(-\frac{3}{2}\frac{\vec{R}^2}{Na^2}\right) \mathrm{d}x\, \mathrm{d}y\, \mathrm{d}z \quad (6)$$

The overall evolution of the complex transverse magnetization is then, not including the homogeneous broadening,

$$M(t) = \mathrm{Re}\left[M_0\left(\frac{3}{2\pi N a^2}\right)^{3/2} \int\int\int \exp\left(\frac{i\Delta k}{2N^2 a^2}(2z^2 - x^2 - y^2)t\right) \exp\left(-\frac{3}{2}\frac{\vec{R}^2}{Na^2}\right) \mathrm{d}x\, \mathrm{d}y\, \mathrm{d}z\right] \quad (7)$$

This yields

$$M(t) = \mathrm{Re}\left[M_0\left(1 - \frac{2}{3} i\Delta N_e^{-1} t\right)^{-1/2}\left(1 + \frac{1}{3} i\Delta N_e^{-1} t\right)^{-1}\right] \quad (8)$$

in which the notation N_e is introduced to include the (constant) factor k: $N_e = N/k$. The time evolution is then expressed as a function of the reduced variable t/N_e, which will be exploited in the sections below.

At short times, $\Delta^2 N_e^{-2} t^2 \ll 1$, $M(t)$ has a Gaussian behavior:

$$M(t) \approx M_0\left(1 - \frac{1}{6}\Delta N_e^{-2} t^2\right) \quad (9)$$

The quantity $\Delta^2 N_e^{-2}/3$ may thus be interpreted as a Van Vleck second moment associated with the residual interactions $\overline{\omega_{IJ}}$. At long times, $\Delta^2 N_e^{-2} t^2 \gg 1$:

$$M(t) \approx (\Delta^2 N_e^{-1} t)^{-3/2} \quad (10)$$

The time evolution of transverse magnetization (eq 5) should be further averaged over the chain length distribution $P(N)$. Thus, at short times (eq 9), N_e^{-2} should be replaced by $\langle N_e^{-2}\rangle$ defined as $\langle N_e^{-2}\rangle = k^2 \int N^{-2} P(N)\, \mathrm{d}N$. Thus, small N_e values are predominant at short times. At long times, eq 10 is replaced by $M(t) \approx \Delta^{-3/2}\langle N_e^{3/2}\rangle t^{-3/2}$, with $\langle N_e^{3/2}\rangle$ defined as $\langle N_e^{3/2}\rangle = k^{-3/2} \int N^{3/2} P(N)\, \mathrm{d}N$. That is, large values of N_e are predominant in this case. Therefore, in a randomly cross-linked system, in which the chain length is broadly distributed, one expects a steeper decrease at short time than in a monodisperse case.

It is emphasized here that this simplified model contains only N_e as an adjustable parameter. As mentioned above, relating N_e to the actual chain length quantitatively would require a detailed investigation of local motions and conformations of the chains, which is beyond the scope of this work. Instead, we show that relative N_e values in different samples with different cross-link densities may be quantitatively compared.

II.2. Dynamics. It has been assumed that intrachain motions are typically faster than 10^{-5} s, which allows one to separate the solid-like and T_2 terms in eq 5. The dynamics of chain fluctuations is reflected in the T_2 term. Though a complete dynamical theory for cross-linked chains has been developed,[20] a simple dependence of this term on the chain length (or equivalently the cross-link density), as that one expressed in eq 4 for the residual interactions, is still difficult to figure out. Moreover, to our knowledge, no systematic NMR measurements investigating quantitatively the N dependence in the T_2 term have been reported so far. For un-cross-linked chains, based on the Rouse model,[23,24] T_2 should decrease as the chain length increases, because the main contribution to T_2 is from the slowest Rouse modes.[20,25,26] The overall N dependence contained in T_2 is generally predicted to be rather weak, however ($T_2^{-1} \approx \ln N$ typically).[25,26] In the case of cross-linked chains, T_2 is significantly shorter than for similar, un-cross-linked chains, because motional restrictions increase (and therefore, T_2 decreases) when the cross-link density increases. This point will not be discussed in more detail in the present work and is left aside for future investigation.

It has been supposed in the previous section that the T_2 term evolves significantly slower than the solid-like term. This point will be demonstrated experimentally (see section IV.1). The ratio between the rates of evolution of both terms is essentially determined by the correlation time of the motions τ_c and should therefore remain of the same order, whatever the particular interaction investigated, provided that the motions are probed at similar frequencies. Following this argument, the liquid-like contribution will not be considered explicitly further on.

III. Experimental Section

NMR experiments were performed on a Bruker MSL spectrometer with a commercial double-resonance static probe at a ^{1}H frequency of 300 MHz. The $\pi/2$ pulse duration could be chosen down to about 2.5 μs for an inner coil diameter of 8 mm. The effect of the cross-link density was investigated in a series of cross-linked poly(styrene-*co*-butadiene) (SBR) samples with different sulfur and accelerator content (Table 1). The unit "phr", or *p*arts per *h*undred *r*ubber, is a relative mass unit and is the common unit for rubber compounding. The polymer SBR 1500 is commercially available ($M_w \approx 300\,000$ g/mol, GPC). It contains the two monomers in a random sequence with a styrene part of 23.5 mol % and a butadiene part of 76.5 mol %.[27] It is a common tire tread material. Besides the polymer the compound contained 3 phr ZnO and 2 phr stearic acid. The degree of cross-linking is determined by the amount of sulfur and accelerator (TBBS, benzothiazyl-2-*tert*-butylsulfenamide) as specified in Table 1. All ingredients were

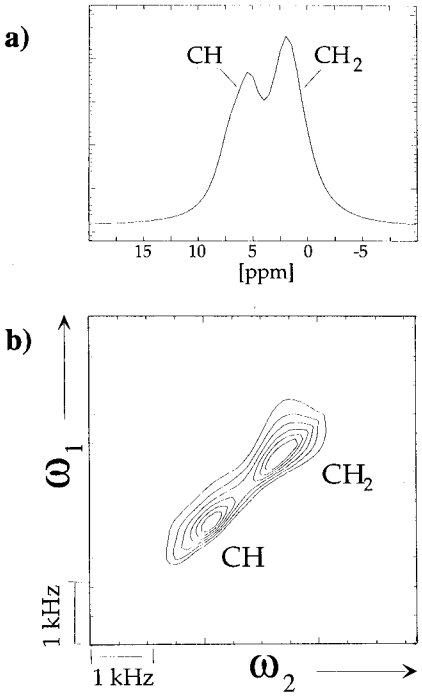

Figure 1. (a) Static ^{1}H NMR spectrum recorded in sample F after a single $\pi/2$ pulse, showing the two lines corresponding to the CH and CH_2 groups. (b) 2D exchange spectrum recorded in sample F with a mixing time of 300 μs. No cross peaks are visible. The ratio of the main axes for the CH_2 peak is ca. 3, which demonstrates the inhomogeneous broadening.

Table 1. Specifications of the SBR Cross-Link Series

sample	sulfur accelerator content (phr)	torque G (dNm)
A	0−0	1
B	0.5−0.5	3.52
C	1−1	5.32
D	1.5−1.5	7.62
E	1−3	7.64
F	2−2	9.53
G	3−1	10.07
H	3−3	12.17
I	4−4	16.5

mixed in a laboratory mixer and vulcanized for 30 min at 160 °C. The degree of cross-linking was measured by the low-frequency shear modulus, or torque, G in the vulcameter after vulcanization, at 160 °C. These measurements were performed on a Monsanto vulcameter MDR-2000-E with an oscillation amplitude of ±0.5° and a measuring frequency of 1.67 Hz. For all NMR experiments the temperature was kept at 20 °C, which corresponds to $T \cong T_g + 70$ K, where T_g is the glass transition temperature for SBR.

IV. Results

IV.I. The Fast-Motion Assumption. The fast-motion assumption is of crucial importance to justify the separation of the fluctuating and residual parts in the Hamiltonian which leads to eq 5. Information on the motions in the range 10^4-10^5 Hz is provided by $T_{1\rho}$. Therefore ^{13}C $T_{1\rho}$ was measured as a function of temperature at a spin-lock field $\omega_1/2\pi = 53$ kHz.[16] A maximum in $T_{1\rho}^{-1}$ was observed at about 263 K, which indicates that, at this temperature, the motions contributing to $T_{1\rho}$ relaxation have correlation times τ_c of the order $\omega_1^{-1} \cong 10^{-4}$ s. These motions are expected to be even faster at room temperature.

The ^{1}H NMR spectrum (Figure 1a) shows two lines corresponding to the CH and CH_2 groups. The CH line contains the contributions from both olefinic and aromatic protons, which are not resolved. ^{1}H two-dimensional (2D) exchange spectra recorded with a short mixing time contain direct information about the solid- or liquid-like (or, in other words, inhomogeneous or homogeneous) character of the line shape.[29−31] Such spectra have been measured for mixing times t_m ranging from 300 μs to a few ms. An example is presented in Figure 1b for $t_m = 300$ μs. In order to destroy the residual transverse magnetization, as well as double quantum coherence terms, a field gradient pulse was inserted after the second $\pi/2$ rf pulse. The gradient pulse duration was 40 μs and the gradient strength was 0.16 T m^{-1}. The diagonal in the 2D spectrum contains the 1D spectrum; cf. Figure 1a. The width of each line along the diagonal reflects both the solid- and liquid-like contributions, i.e. the homogeneous and inhomogeneous broadening, whereas the width perpendicular to the diagonal reflects selectively the liquid-like (or homogeneous) line width only, since no exchange is expected to take place for such a short mixing time. For both lines the widths measured in both directions are clearly different. This demonstrates that the line is inhomogeneously broadened, or, in other words, contains a solid-like contribution. The ratio between inhomogeneous and homogeneous line widths is typically 3, as measured at half-height on the CH_2 line.

Additionally, it was found that no cross-peaks appear in the 2D exchange spectrum for mixing times up to 3 ms. This proves that the different groups, i.e. CH and CH_2, are effectively isolated on this time scale, which covers the entire evolution curves investigated further on. This provides another justification for the two-spin approximation underlying eqs 4 and 8.

Further evidence for the inhomogeneous broadening of the line is the appearance of solid echoes in a solid−echo pulse train, or OW4 pulse sequence,[32,33] which refocuses residual dipolar interactions. The pulse sequence is $(\pi/2_x,(\tau,\pi/2_y,\tau)_n)$. A solid echo is generated between each pair of $\pi/2_y$ pulses. The solid echo intensity decays exponentially with an effective relaxation rate T_{2e} given by[34,35]

$$T_{2e}^{-1} = \frac{\overline{\omega^2} J(0)}{4}\left[1 - \frac{\tanh(\tau/\tau_c)}{\tau/\tau_c}\right] \qquad (11)$$

in which τ_c is the correlation time of the motions which contribute to the relaxation. $J(0)$ is the spectral density at zero frequency. $\overline{\omega^2}$ is the second moment associated with the residual interactions. Interactions which are linear in the spin operator I_z, i.e. the chemical shifts and field inhomogeneities, are only partially refocused in the OW4 sequence. Thus, if the signal is not exactly on resonance, the OW4 sequence will act as a (partial) chemical shift filter and part of the magnetization will be lost at short times.

As well as in the 2D exchange spectrum presented above, the homogeneous and inhomogeneous contributions may be observed separately in this time-domain experiment.[36] T_{2e} becomes independent of the pulse delay τ in the limit of fast motions, i.e. $\tau/\tau_c \gg 1$. In this case, T_{2e} is similar to the T_2 relaxation time. Thus, the time scale of the motions which contribute to the ^{1}H transverse relaxation may be probed, in order to check the fast motion assumption underlying eq 5. An additional semiquantitative test of the fast-motion assumption is provided from eq 11 by the T_{2e} value itself via the relation $T_{2e}^{-1} \cong \overline{\omega^2} J(0) \cong \overline{\omega^2}\tau_c$. Since residual

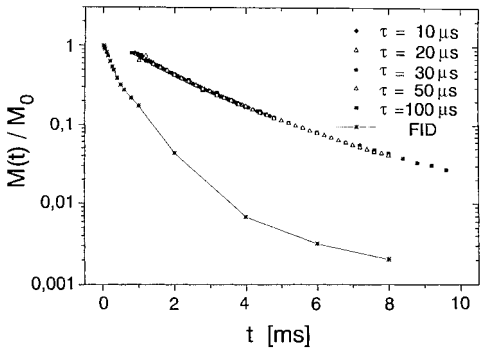

Figure 2. ^{1}H transverse relaxation during a solid echo pulse train in sample F for different values of the pulse delay τ ranging from 10 to 100 μs. The plot is on a logarithmic scale. The solid echo curves are compared with the magnetization decay obtained as the envelope of echoes obtained in a standard spin−echo pulse sequence (chemical shift demodulated FID) in the same sample: All solid echo curves are superimposed to show that the decay rate $1/T_{2e}$ is independent of τ.

interactions may be estimated from the solid-like term, the correlation time τ_c may in principle be estimated from this experiment.

In Figure 2 the decays obtained in a solid echo train sequence are plotted for different values of the delay τ between pulses, in sample F (see section III and Table 1). The values vary between 10 and 100 μs. The $\pi/2$ pulse duration is 2.8 μs. The curves represent the signal intensity at the echo maximum after an incremented number of pulses in the train. Thus, the chemically shifted lines are not resolved. The resonance frequency is chosen in between the two lines corresponding to the CH and CH_2 groups, which are separated by about 3.35 ppm. Therefore, part of the magnetization is lost at short times, due to the chemical shift filter effect mentioned above. Apart from that, the magnetization decay is indeed independent of the pulse delay τ.

The solid echo decay is significantly slower than the decay obtained in a spin−echo pulse sequence (cf. Figure 2). The ratio of these two decay rates corresponds to the ratio of homogeneous to inhomogeneous broadening which was measured in the 2D exchange spectrum in Figure 1b.

The different decays were normalized so that the long-time parts superpose exactly. According to eq 11, this superposition for different τ delays is a clear indication that the motions are in the fast regime, $\tau/\tau_c \gg 1$. T_{2e} values range between 2.5 and 5 ms, and the value of the second moment $\overline{\omega^2}$, related to the overall width of the spectrum at half-height, is of the order 3×10^7 s^{-2}, which gives τ_c in the range 10^{-6}−10^{-5} s, according to $T_{2e}^{-1} \cong \overline{\omega^2}\tau_c$. This justifies the assumption that intra-chain motions are fast.

IV.2. ^{13}C-Edited ^{1}H Transverse Relaxation. This experiment is similar to the wide-line separation (WISE) technique used in solid-state NMR to investigate site-resolved molecular mobilities.[19,28,37,38] ^{1}H transverse magnetization is created by a single $\pi/2$ pulse and then transferred to ^{13}C by a cross-polarization pulse of fixed length after a variable evolution time t, and the ^{13}C signal is then observed under standard ^{1}H decoupling. This experiment has two major advantages. First, the signals from different groups (namely, the CH and CH_2 groups) are well resolved. Then, provided that a short contact time is used in order to avoid ^{1}H spin diffusion, only ^{1}H atoms directly bonded to ^{13}C atoms are observed and the proton transverse relaxation is governed by a very specific dipolar interaction, namely the ^{1}H−^{13}C heteronuclear coupling.

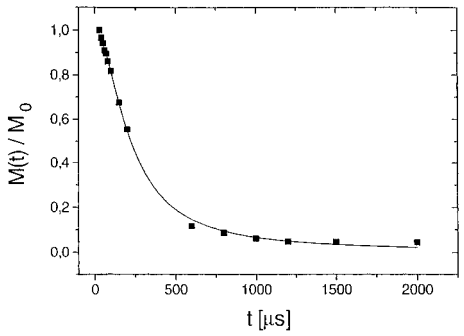

Figure 3. Fit of the ^{13}C-edited ^{1}H transverse relaxation of the CH group in sample F using eq 8. The best fit is obtained for the fitting parameter value $N_e = 11.55$ in this case.

In the case of CH groups, the static ^{1}H−^{13}C heteronuclear interaction is given by

$$\omega_{HC} = -\Delta_{HC}\frac{3\cos^2\vartheta - 1}{2} \qquad (12)$$

in which Δ_{HC} is given by an equation similar to eq 3: $\Delta_{HC} = r^{-3} \times 1.887 \times 10^5$ rad·s^{-1} with r in Å. For the CH group, $r = 1.1$ Å and $\Delta_{HC} = 1.42 \times 10^5$ rad·s^{-1}. The ^{1}H transverse relaxation for the CH group is then given by an equation identical to eq 8.

The T_2 contribution is neglected here. Note also that at long times ($\Delta_{HC}^2 N_e^{-2} t^2 \gg 1$), interactions between the CH and CH_2 groups, which are weaker but not averaged to zero, may contribute to the time evolution.

In the ^{13}C frequency dimension, the CH and CH_2 groups are separated by about 100 ppm.[28] Olefinic and aromatic carbons cannot be resolved. The ^{13}C-edited ^{1}H transverse relaxation for the CH group is the NMR observable which can be analyzed in the most precise way, because the time evolution is governed by the heteronuclear dipolar coupling within isolated CH groups. Thus, instead of using small and long-time expansions and/or asymptotic behaviors, we choose to fit the experimental decays over the entire time range with one single function, related to the simple model recalled in section II and given in eq 8. This means that the chain length distribution is actually neglected.

Figure 3 gives an example of fit against eq 8. A $\pi/2$ pulse of 3.7 μs and a contact time of 1.3 ms were used. It shows that the computed function provides a very good representation of the experimental decay over the entire time range, with only one adjustable parameter N_e. This is an additional indication of the relevance of this approach. It shows that the spin pair model is a reasonable approximation, especially for the initial part of the decay, and it also suggests that the Gaussian distribution given in eq 6 is a reasonable representation of the constraints on a molecular scale.

Relaxation curves for three samples with different cross-link densities are plotted in Figure 4a as functions of the time t. As expected, the decay is faster for higher cross-link density. From the fit against eq 8, a value for the N_e factor is determined for each sample. The ^{13}C-edited ^{1}H transverse relaxation curves for the CH group are plotted as a function of the reduced variable t/N_e in Figure 4b for the previous three samples and in Figure 4c for all the samples in the series to illustrate the accuracy of the scaling property.

The pertinence of the N_e parameter which is found in this way also manifests itself in the time evolution

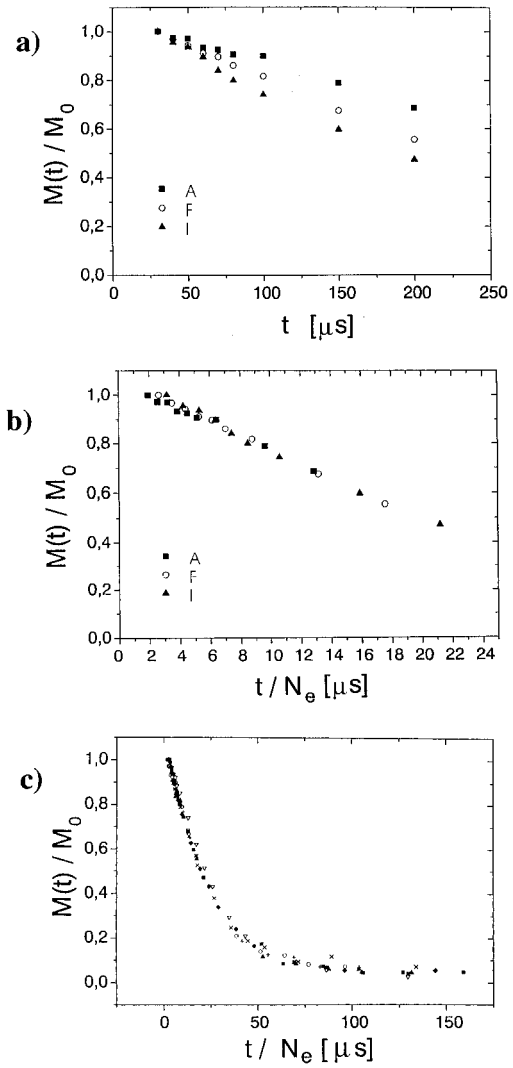

Figure 4. (a) The ^{13}C-edited ^{1}H transverse relaxation curves of the CH group for three different samples in the series as a function of time t. (b) Rescaling of the time axis superposes the three curves. (c) ^{13}C-edited ^{1}H transverse relaxation curves of the CH group for all samples in the series plotted as a function of the reduced variable t/N_e. All curves superpose so that a master curve is obtained.

of the ^{13}C-edited ^{1}H transverse relaxation measured without chemical resolution, i.e. the superposition of the CH and CH_2 signals. These time relaxation curves are also expressed as a single function of the reduced variable t/N_e. In Figure 5, the ^{13}C-edited ^{1}H relaxation curves for all samples in the series are plotted against t/N_e. For short times, all curves superpose, so that a master curve is obtained.

IV.3. Chemical versus Physical Cross-Links. The N_e values obtained in all samples of the series range from about 9 at the higher cross-link density to 16 in the un-cross-linked sample. They are plotted in Figure 6 versus the maximum vulcameter torque G. The torque G is used as an independent measure of the cross-link density, according to the standard relation $G \cong nk_BT \propto N^{-1}k_BT$,[18] in which n is the cross-link density, i.e. the number of cross-linked chains per unit volume.[39] The curve shown in Figure 6 may be considered as roughly linear. However, it does not cross the origin, which means that although the torque vanishes in a non-cross-linked sample, the NMR transverse relaxation is still largely solid-like. As noted above, this is a clear illustration of the restrictions of the chain dynamics by

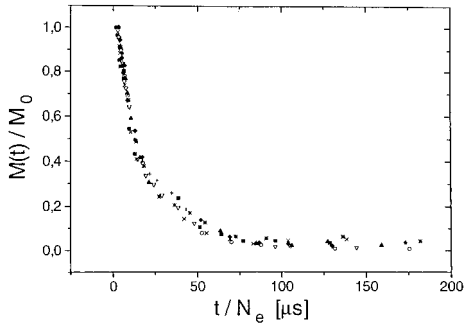

Figure 5. ^{13}C-edited ^{1}H transverse magnetization relaxation curves for the CH and CH_2 groups as a function of the reduced variable t/N_e for all samples of the series. A master curve is obtained.

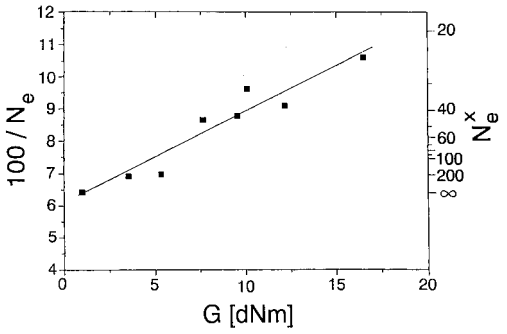

Figure 6. Inverse of the parameter N_e, obtained in each sample by fitting the ^{13}C-edited ^{1}H relaxation of the CH group as illustrated in Figure 2 plotted versus the mechanical torque G. The parameter $(N_e^X)^{-1}$ is obtained by subtracting the offset $(N_e^0)^{-1}$, which represents the contribution from physical cross-links. On a reciprocal scale, the corresponding N_e^X values are also displayed.

nonpermanent physical cross-links which are also present in an un-cross-linked polymer melt and are not mechanically active in the vulcameter measurements.[12]

The effective density of physical cross-links probed by NMR relaxation, or equivalently the average chain length between them, N_e^0, is given by the N_e value measured in the un-cross-linked sample, $N_e^0 \cong 16$ (cf. Figure 6). Thus, considering the value $N_e^0 \cong 16$ to be constant throughout the whole series, the average length between actual chemical cross-links N_e^X may be estimated by the simple equation $N_e{}^{-1} = (N_e^0)^{-1} + (N_e^X)^{-1}$, which assumes that the contributions to residual dipolar coupling are additive (cf. eq 8). The values of N_e^X obtained in this way range from about 25 (higher cross-link density) to 200 (lower density). They are reported in Figure 6. It is worth noting that N_e^X is larger than N_e^0 for the whole series. Thus, the residual dipolar coupling due to physical cross-links is larger than that resulting from chemical cross-links.

It is interesting at this point to compare the present values to those in semicrystalline polyethylene (PE) deduced via simulations aimed at interpreting deuteron NMR line shapes.[12,40] In that case, the amorphous parts of the chains are fixed to the crystallites. It was found that for PE chains with fixed ends, with a mean-squared end-to-end distance of the order the Gaussian value Na^2, the residual second moment is about 0.4% of the static one for chains of $N = 13$ repeat units or longer, which in our notation corresponds to an N_e value of the order 16. This value is therefore in remarkable agreement with our estimate. This implies that the parameter k introduced in eq 4 is actually of the order unity. A

comparable value in terms of the number of repeat units between physical cross-links was also found in *cis*-1,4-polybutadiene.[11] The macroscopic anisotropy induced upon stretching cross-linked elastomers also depends on the density of physical and chemical cross-links. Indeed it was found in a series of poly(dimethylsiloxane) elastomers with a constant density of cross-links but different densities of trapped entanglements that the anisotropy measured by deuterium NMR is sensitive to entanglements.[41,42] Dangling chains may of course be present and have NMR properties different from that of cross-linked ones. However, no purely liquid-like contribution due to dangling chains was introduced in any of the experiments presented here. Since the precursor chains are very long, the fraction of dangling chains is probably low.

IV.4. ^{1}H Transverse Decay Obtained in a Spin−Echo Pulse Sequence. To confirm the scaling property demonstrated above, different experiments have been performed, aimed at investigating different dipolar couplings within the chains. They are presented in this and the following subsections. First, the evolution of the transverse magnetization after a single $\pi/2$ pulse was observed by the standard spin−echo sequence. Chemical shifts are refocused by this pulse sequence. Thus, the signal obtained is the "chemical-shift-demodulated FID", that is, the superposition of the signals from both CH and CH_2 groups, evolving under the influence of dipolar interactions only.

Figure 7a shows chemical-shift-demodulated ^{1}H transverse magnetization relaxation for the different samples in the series plotted as a function of the reduced variable t/N_e. No attempt is made to fit these decays to eq 8, because the spin pair approximation is difficult to justify here. Although the largest interaction is the ^{1}H−^{1}H coupling within a CH_2 group, all ^{1}H−^{1}H dipolar interactions within one chain segment also contribute to the time evolution. It appears immediately that all relaxation functions superpose, giving a master curve. This scaling property means that the isolated spin group approximation is justified within the time range of this decay. In other words, interactions between protons belonging to remote segments give a negligible contribution to the time evolution. It is interesting to note that the decay rates of the ^{1}H transverse relaxation are of the same order as those of the ^{13}C-edited ^{1}H transverse relaxation (see Figure 5). This is due to the fact that the respective dipolar interactions are of the same order: $\gamma_H^2 r_{HH}^{-3} \approx \gamma_H \gamma_C r_{HC}^{-3}$ with $r_{HH} \approx 1.8$ Å and $r_{HC} \approx 1.1$ Å.

IV.5. Rate of ^{1}H Longitudinal Magnetization Exchange from CH to CH_2 Groups. The interaction which is probed here is the dipolar coupling between one CH and one CH_2 group within a butadiene monomer. The pulse sequence is similar to the standard NOE sequence used for probing connectivities in multidimensional NMR:[43] $(\pi/2_x,\tau,\pi/2_{-x},t_m,\pi/2)$, used here in a one-dimensional way. The delay τ is chosen in order to produce a chemical shift filter, in which the magnetization of the CH groups is selected and then transferred back to longitudinal magnetization by the second pulse. The signal is then observed after a variable mixing time t_m.

From the NMR point of view, this experiment is more complicated, since the interaction here is not a two-spin interaction, and both groups (CH and CH_2) are separated by a chemical shift which is of the same order of magnitude as the residual dipolar couplings involved.

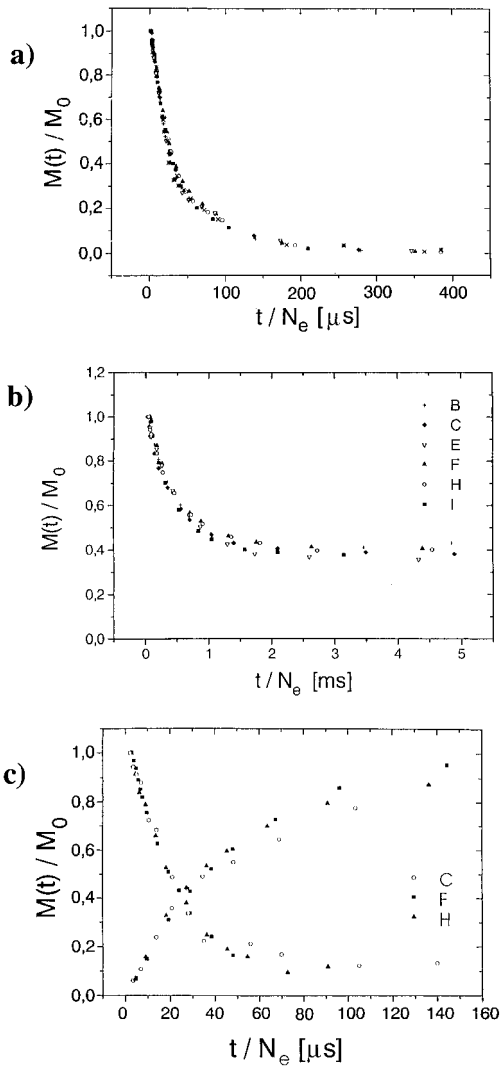

Figure 7. (a) ^{1}H transverse magnetization relaxation curves for all samples in the series as a function of the reduced variable t/N_e. (b) Rates of ^{1}H magnetization transfer from the CH to CH_2 groups for the different samples of the series as functions of the reduced variable t/N_e. The curves have been corrected for T_1 relaxation. (c) Evolution of the ^{13}C magnetization in the CH groups in a cross-polarization experiment as a function of the reduced variable t/N_e in different samples of the series (rising curves). The curves were corrected for $T_{1\rho}$ relaxation. The ^{13}C-edited ^{1}H magnetization relaxation curves for the CH groups are also plotted for comparison of the initial evolution rates (falling curves).

Therefore we consider only the short-time behavior of the magnetization exchange.[19] In analogy to this equation, it may be expected that at short times the effective interaction responsible for the magnetization exchange is the residual dipolar coupling $\bar{\omega}$ between the CH and CH_2 groups. A detailed description of this process will be published later.[44] Within one monomer, this coupling is not averaged to zero by fast chain motions, but the distance r between the groups is averaged by local configurational jumps to an average value r_0.

For short mixing times t_m, the evolution of the filtered CH signal can be described by

$$M_z(t_m) = M_z(0)\left(1 - \frac{1}{2}\langle\bar{\omega}^2\rangle t_m^2\right) \qquad (13)$$

We then assume that the interaction obeys the same scaling property as expressed in eq 4, so that eq 13 is in fact similar to eq 9 at short times.

^{1}H longitudinal magnetization exchange curves from CH to CH_2 groups are plotted as a function of the reduced variable t/N_e in Figure 7b for the different samples of the series. The $\pi/2$ pulse duration was 3 μs and the delay τ for the chemical shift filter was 280 μs. The curves were corrected for T_1 relaxation by fitting the long-time part to $\exp(-t/T_1)$. The curves were then normalized to the same initial value. The same T_1 value was used to correct all curves, since it is expected that T_1 does not depend on the cross-link density at high frequency. A master curve is obtained in this case as well.

IV.6. Rate of Magnetization Transfer from ^{1}H to ^{13}C. In a cross-polarization (CP) experiment using the spin-locking procedure,[45] the process of polarization transfer from abundant spins (^{1}H) to rare spins (^{13}C) depends on the nature of the system under study. In a rigid solid with a dominant, distinct, heteronuclear dipolar coupling, the polarization transfer between two spins during a cross-polarization pulse is governed by the effective heteronuclear dipolar Hamiltonian:

$$H_{HC} = \omega_{HC}(I_z^H I_z^C + I_y^H I_y^C) \tag{14}$$

where ω_{HC} is defined as in eq 12. The evolution of the transverse magnetization during a cross-polarization contact pulse is described by[19]

$$I_x^H \xrightarrow{H_{HC}} \frac{1}{2}(1 + \cos \omega_{HC}t)I_x^H + \frac{1}{2}(1 - \cos \omega_{HC}t)I_x^C + \sin \omega_{HC}t(I_y^H I_z^C - I_z^H I_y^C) \tag{15}$$

In a many-body rigid spin system, for times longer than the correlation time of the dipolar fluctuations, the transient oscillations apprent in eq 15 are absent and the CP process can be described by a thermodynamic equation with a rate $T_{HC}^{-1} \cong M_{2,HC}\tau_d$, where $M_{2,HC}$ is the heteronuclear Van Vleck second moment and τ_d is the correlation time of the dipolar fluctuations.[16,46]

In elastomers, static, isolated, residual dipolar couplings are present, with only intragroup interactions being effective. In the fast-motion regime, the evolution may therefore be described by an equation analogous to eq 15:

$$I_x^H \xrightarrow{H_{HC}} \frac{1}{2}e^{-t/T_{1\rho}^H}(1 + \langle e^{-t/T_{2CP}} \cos \overline{\omega_{HC,\vec{R}}}t\rangle)I_x^H + \frac{1}{2}e^{-t/T_{1\rho}^C}(1 - \langle e^{-t/T_{2CP}} \cos \overline{\omega_{HC,\vec{R}}}t\rangle)I_x^C \tag{16}$$

in which $\overline{\omega_{HC,\vec{R}}}$ is the residual interaction defined for each chain by eq 4, and the average denoted by $\langle ... \rangle$ is an ensemble average as defined in eq 7. Then, the CP evolution is of the solid-like (or inhomogeneous) type, similar to the ^{1}H transverse magnetization evolution. Transient oscillations are of course damped by the effect of disorder in the system. The T_{2CP} relaxation term contains both the influence of the fluctuating part of the Hamiltonian which describes the dominant interaction H_{HC} and the effect of other dipolar couplings.

The time evolution of ^{13}C magnetization in the CH group during cross-polarization is plotted as a function of the reduced variable t/N_e in Figure 7c (rising curves) for different samples in the series. The field strength of the cross-polarization pulse was $\omega_1/2\pi = 42$ kHz. The curves were corrected for $T_{1\rho}$ relaxation by fitting the long-time part of the curves with $\exp(-t/T_{1\rho})$. However, the normalization in this series of curves is difficult, because it was difficult to measure the absolute intensity of the signal. The scattering of the different curves in Figure 7c may actually be due to normalization uncertainties and does not preclude the validity of the t/N_e scaling property in this case. Note finally that the interaction which determines the spin evolution in this case is exactly the same as in the observation of ^{13}C-edited ^{1}H transverse magnetization relaxation for short enough contact times. Thus the evolution rates which are observed in each case should be equal, at least for short evolution times. The ^{13}C-edited ^{1}H magnetization relaxation curves for the CH groups are also plotted in Figure 7c (falling curves). It is clear that the initial evolution rates in both experiments are indeed similar.

V. Conclusions

In this work, a series of SBR elastomers with different cross-link densities was studied by NMR. Local motional anisotropy due to chemical and physical cross-links leads to residual dipolar interactions and thus to solid-like time evolution for the NMR observables investigated, or, equivalently, to inhomogeneous line broadening. Various NMR experiments probing these residual dipolar couplings in different ways were correlated using this concept. The concordance in the results of all these experiments is a clear demonstration of the pertinence of this approach. The simple model adopted here to describe the polymer chains relies on the assumption that local chain motions are fast,[47] which in turn leads to the assumption that pairs of spins are effectively isolated. For this assumption to be valid, one must perform the NMR experiments at temperatures far enough above T_g. To our knowledge, this is the first time that 2D exchange spectra with a very short mixing time are used to demonstrate in a direct way the solid-like (or inhomogeneous) character of the line shape in elastomers. It also proves that the chemical groups are effectively isolated on the time scale covered in all the experiments presented herein. The correlation times of the motions are probably also affected by the cross-link density, but the effect of this on the NMR observables considered here is minor, except when specially designed, multiple pulse sequences are used to refocus residual interactions.

The effect of the densities of both physical cross-links and chemical cross-links was expressed by one adjustable parameter N_e. All NMR quantities investigated reflect the same scaling property of the residual dipole−dipole interactions. This leads to master curves including all samples in the series when the time evolution curves are plotted as a function of the reduced variable t/N_e. It was shown that, even in the higher cross-linked sample, the dominant contribution to the residual dipole−dipole interactions results from physical cross-links. Such transient constraints are also present in polymer melts and have to be taken into account for interpreting relaxation data in such systems.[48−50]

The use of the solid-like concept to characterize technical elastomers of different types thus allows a wide flexibility, and therefore perhaps a wide applicability of this type of NMR measurements. Though the different NMR observables investigated here contain essentially the same dependence upon the cross-link density, one should choose the most selective and convenient experiment for each particular question posed. This point is also important for NMR imaging of elastomers. There, it is essential to select the NMR

observables providing the best contrast, i.e. sensitivity either to the spatial variations of cross-link density in inhomogeneous samples or to the spatial distribution of local constraints in macroscopically stressed samples. Specifically, the t/N_e scaling property of the NMR decays clarifies why the contrast in imaging experiments is generally better when the signal is monitored after long evolution times. In carrying out imaging experiments, one has to compromise between obtaining strong signal (at short evolution times) and achieving good contrast (at long evolution times).

Acknowledgment. P.S. acknowledges the support of a CNRS/MPG cooperation program. C.F. acknowledges financial support from the Deutsche Kautschuk Gesellschaft e.V. He also thanks Dr. K. Unseld and coworkers, SP Reifenwerke GmbH, Hanau, for providing the samples and for many helpful discussions.

References and Notes

(1) Koenig, J. L. *Spectroscopy of Polymers*; ACS Professional Reference Book; American Chemical Society: Washington, DC, 1992.
(2) Blümich, B.; Kuhn, W., Eds. *Magnetic Resonance Microscopy, Methods and Applications in Materials Science, Agriculture and Biomedicine*; VCH Publishers: Weinheim, 1992.
(3) Fedotov, V. D.; Schneider, H. Structure and Dynamics of Bulk Polymers by NMR Method. In *NMR, Basic Principles and Progress*; Springer: Berlin, 1989; Vol. 21.
(4) Cohen-Addad, J. P. NMR and Fractal Properties of Polymeric Liquids and Gels. In *Progress in NMR Spectroscopy*; Emsley, J. W., Feeney, J., Sutcliffe, L. H., Eds.; Pergamon Press: Oxford, 1993.
(5) Kenny, J. C.; McBrierty, V. J.; Rigbi, Z.; Douglass, D. C. *Macromolecules* **1991**, *24*, 436.
(6) Kuhn, W.; Barth, P.; Hafner, S.; Simon, G.; Schneider, H. *Macromolecules* **1994**, *27*, 5773.
(7) Cohen-Addad, J. P.; Vogin, R. *Phys. Rev. Lett.* **1974**, *33*, 940.
(8) Cohen-Addad, J. P. *J. Chem. Phys.* **1974**, *60*, 2440.
(9) Cohen-Addad, J. P.; Viallat, A.; Huchot, Ph. *Macromolecules* **1987**, *20*, 2146.
(10) Kulagina, T. P.; Litvinov, V. M.; Summanen, K. T. *J. Polym. Sci., Part B: Polym. Phys.* **1993**, *31*, 241.
(11) Cohen-Addad, J. P. *J. Chem. Phys.* **1975**, *63*, 4880.
(12) Collignon, J.; Sillescu, H.; Spiess, H. W. *Colloid Polym. Sci.* **1981**, *259*, 220.
(13) Spiess, H. W. *Colloid Polym. Sci.* **1983**, *261*, 193.
(14) Sotta, P.; Deloche, B. *Macromolecules* **1990**, *23*, 1999.
(15) Macinko, J. J.; Parker, A. A.; Rinaldi, P. L.; Ritchey, W. M. *Polym. Mater. Sci. Eng.* **1993**, *68*, 266.
(16) Fülber, C.; Demco, D. E.; Blümich, B. *Solid State Nucl. Magn. Reson.*, accepted.
(17) Kimmich, R.; Schnur, G.; Köpf, M. *Prog. NMR Spectrosc.* **1988**, *20*, 385.
(18) Treloar, L. R. G. *The Physics of Rubber Elasticity*; Clarendon Press: Oxford, 1975.
(19) Schmidt-Rohr, K.; Spiess, H. W. *Multidimensional Solid-State NMR and Polymers*; Academic Press: London, 1994.
(20) Brereton, M. *Macromolecules* **1989**, *22*, 3667; **1991**, *24*, 2068.
(21) Gronski, W.; Stadler, R.; Jacobi, M. M. *Macromolecules* **1984**, *17*, 741.
(22) Sandakov, G. I.; Smirnov, L. P.; Sosikov, A. I.; Summanen, K. T.; Volkova, N. N. *J. Polym. Sci., Part B: Polym. Phys.* **1994**, *32*, 1585.
(23) Rouse, P. E. *J. Chem. Phys.* **1953**, *21*, 1272.
(24) Ward, I. M. *Mechanical Properties of Solid Polymers*; John Wiley & Sons: Chichester, 1971.
(25) Ullman, R. *J. Chem. Phys.* **1965**, *43*, 3161.
(26) Brereton, M. *Macromolecules* **1990**, *23*, 1119.
(27) Brydson, J. A. *Rubber Chemistry*; Applied Science Publishers: London, 1978.
(28) Fülber, C.; Demco, D. E.; Weintraub, O.; Blümich, B. *Macromol. Chem. Phys.*, in press.
(29) Aue, W. P.; Bartholdi, E.; Ernst, R. R. *J. Chem. Phys.* **1976**, *64*, 2229.
(30) Zemke, K.; Schmidt-Rohr, K.; Spiess, H. W. *Acta Polym.* **1994**, *45*, 148.
(31) Jäger, C.; Feike, M.; Born, R.; Spiess, H. W. *J. Non-Cryst. Solids* **1994**, *180*, 91.
(32) Ostroff, E. D.; Waugh, J. S. *Phys. Rev. Lett.* **1966**, *16*, 1097.
(33) Mansfield, P.; Ware, D. *Phys. Rev.* **1968**, *168*, 318.
(34) Schmiedel, H.; Freude, D.; Gründer, W. *Phys. Lett.* **1971**, *34A*, 162.
(35) Ursu, I.; Balibanu, F.; Demco, D. E.; Bogdan, M. *Phys. Status Solidi B* **1986**, *136*, 309.
(36) Cohen-Addad, J. P. *Phys. Rev. Lett.* **1995**, *74*, 3820.
(37) Zumbulyadis, N. *Phys. Rev. B* **1986**, *33*, 6495.
(38) Schmidt-Rohr, K.; Clauss, J.; Spiess, H. W. *Macromolecules* **1992**, *25*, 3273.
(39) Fülber, C.; Unseld, K.; Herrmann, V.; Jacob, K. H.; Blümich, B. *Colloid Polym. Sci.* **1996**, *274*, 191.
(40) Rosenke, K.; Sillescu, H.; Spiess, H. W. *Polymer* **1980**, *21*, 757.
(41) Dubault, A.; Deloche, B.; Herz, J. *Polymer* **1984**, *25*, 1405.
(42) Dubault, A.; Deloche, B.; Herz, J. *Macromolecules* **1987**, *20*, 2096; **1990**, *23*, 2823.
(43) Ernst, R. R.; Bodenhausen, G.; Wokaun, A. *Principles of Nuclear Magnetic Resonance in One and Two Dimensions*; Clarendon Press: Oxford, 1987.
(44) Demco, D. E.; Hafner, S.; Fülber, C.; Graf, R.; Spiess, H. W., in preparation.
(45) Mehring, M. *High Resolution NMR in Solids*, 2nd ed., Springer-Verlag: Berlin, 1983.
(46) Demco, D. E.; Tegenfeldt, J.; Waugh, J. S. *Phys. Rev. B* **1975**, *11*, 4133.
(47) Samulski, E. T. *Polymer* **1985**, *26*, 177.
(48) Schweizer, K. S. *J. Chem. Phys.* **1989**, *91*, 5802.
(49) Schweizer, K. S. *J. Chem. Phys.* **1989**, *91*, 5822.
(50) Fatkullin, N.; Kimmich, R. *J. Chem. Phys.* **1994**, *101*, 822.

MA960141E